Scientific Contributions Oil & Gas, Vol. 48. No. 4, December: 175 -186

**SCIENTIFIC CONTRIBUTIONS OIL AND GAS**

**Testing Center for Oil and Gas**
**LEMIGAS**

Journal Homepage:http://journal.lemigas.esdm.go.id
ISSN: 2089-3361, e-ISSN: 2541-0520

# Enhancing Subsurface Geological Model Resolution in Challenging Seismic Conditions by Using Model-Based Deterministic Inversion

Abi Mawalid[1], Abdul Haris[1], and Edy Wijanarko[2]

[1]Department of Physics, FMIPA Universitas Indonesia
Lingkar Street, Pondok Cina, Beji Sub-district, Depok City, West Java, Indonesia.

[2]Testing Center for Oil and Gas LEMIGAS
Ciledug Raya Street Kaveling 109, Cipulir, Kebayoran Lama, South Jakarta, Indonesia.

Corresponding Author : Abi Mawalid (abimawalid10@gmail.com)

Manuscript received: January 16th, 2026; Revised: February 10th, 2026
Approved: February 13th, 2026; Available online: March 12th, 2026; Published: March 12th, 2026.

**ABSTRACT** - The limited resolution of 2D seismic data often limits the accuracy of subsurface interpretation. This study explores how deterministic inversion enhances the elastic representation of low-resolution intervals in Field X and contributes to more precise reservoir interpretation. By applying deterministic inversion, this study aims to improve the mapping of lithological variations throughout the interval. Petrophysical data show that the target zone contains porosity values of 11–22%, Gamma Ray readings of 10–120 API, and P-impedance values of 11022–15343. These parameters support well–seismic tying and model calibration. The inversion generates an acoustic impedance model that closely aligns with the log trends and shows a coherence error of only 6.23% within the target interval. Domains with increased permeability and reduced GR readings appear as subtle impedance irregularities, whereas more consolidated phases show higher impedance. The resulting impedance response captures geologically meaningful mid-range lithological variations, although limitations in seismic resolution still reduce the precision of stratigraphic delineation. Overall, the findings demonstrate that careful calibration with petrophysical datasets provides a consistent and quantifiable impedance framework, even in areas with limited seismic fidelity, thereby supporting more reliable reservoir interpretation.

**Keywords**: deterministic inversion, acoustic impedance, low-resolution seismic data.



**How to cite this article:**

Abi Mawalid, Abdul Haris, and Edy Wijanarko, 2026, Enhancing Subsurface Geological Model Resolution in Challenging Seismic Conditions by Using Model-Based Deterministic Inversion, Scientific Contributions Oil and Gas, 49 (1) pp. 175-186. DOI org/10.29017/ scog.v49i1.1976.

## INTRODUCTION

Seismic inversion is commonly used in reservoir characterization because it provides quantitative elastic properties that can't be directly obtained from reflection seismic data. (Russell, B. H. 1988). Advances in inversion workflows, including improvements in wavelet extraction and log seismic calibration, have contributed to more consistent geological interpretation, although their effectiveness still heavily depends on the quality, bandwidth, and vertical resolution of the seismic data (Avseth, P., Mukerji, T., & Mavko, G. 2005).

Challenges become more evident in settings like X Field, where the seismic data have limited bandwidth and weak impedance contrasts. These conditions reduce the capability of deterministic inversion to resolve fine geological details and often result in overly smoothed impedance models, particularly in clastic environments (Grana, D., & Della Rossa, E., 2010). Although various inversion workflows have been refined to enhance structural and stratigraphic imaging, their performance is still fundamentally limited when applied to seismic datasets with inherently narrow bandwidth and high noise levels (HRS 2011).

Despite these challenges, deterministic inversion remains a viable method in data limited settings, as it allows for the integration of low frequency trends from well logs and offers a stable, transparent solution and computationally efficient workflow (H. Wu 2015). The single best estimate impedance model it generates is invaluable for supporting structural and stratigraphic interpretation, particularly when clear representation of subsurface continuity is required (Grana, D. 2017).

Based on these considerations, this study applies a deterministic inversion workflow incorporating well logs, extracted wavelets, and model-based constraints to generate an acoustic impedance model for the target interval. The expected outcomes include better delineation of reservoir intervals, despite limitations in seismic resolution, and clearer insights into the applicability of deterministic inversion in environments with data quality constraints.

## METHODOLOGY

This section outlines the workflow for implementing deterministic seismic inversion using the Hampson Russell Suite (HRS). Deterministic inversion is widely applied in seismic reservoir studies due to its well-defined computational structure and its ability to generate stable acoustic impedance models directly constrained by seismic and well-log data. Among the available deterministic approaches, such as recursive inversion, sparse- spike inversion, and model-based inversion, the modelbased method was chosen as the most suitable for the Field X seismic dataset. This choice was driven by its ability to incorporate prior geological information and provide a controlled framework for matching seismic amplitudes.

Deterministic seismic inversion in this study follows the classical convolutional model, where the recorded seismic trace is represented as the convolution between the embedded wavelet and the earth's reflectivity:

$$s(t) = w(t) * r(t) \quad (1)$$

This formulation shows that s(t) is the observed seismic signal, generated by applying the source wavelet w(t) to the reflectivity series r(t), which represents impedance contrasts in the subsurface (Robinson, E. A., & Treitel, S. 2000). The wavelet was extracted statistically in the frequency domain using

$$W(\omega) = \sqrt{S(\omega)} \quad (2)$$

where W(ω)) denotes the estimated wavelet, and S (ω) is the averaged seismic amplitude spectrum. The square root operation ensures that the wavelet remains amplitude consistent and phase-stable for well seismic calibration (Yilmaz, Ö. 2001). Reflectivity at well locations was calculated using the two-layer impedance contrast

$$R = \frac{Z_2 - Z_1}{Z_2 + Z_1} \quad (3)$$

where $Z_1$ and $Z_2$ are the acoustic impedances of adjacent layers. This relationship determines both the polarity and strength of reflections, ensuring the accurate generation of synthetic seismograms following check shot correction (Sheriff, R. E., & Geldart, L. P. 1995).

In practical geophysical workflows, Model-Based Inversion is typically carried out using the Generalized Linear Inversion (GLI) framework, which updates the initial subsurface impedance model in an iterative manner to minimize the misfit between the synthetic and the observed seismic responses. In this formulation, the forward seismic modeling operator is linearized, allowing the recorded seismic trace to be represented as a convolutional or matrix-based linear relationship with changes in acoustic impedance. This linearized representation enables the inversion algorithm to solve for impedance variations directly, while progressively refining the model to achieve convergence toward the measured data (Russell, B. H. 1988).

$$F(M) \approx F(M_0) + G\Delta M \quad (4)$$

where $M_0$is the initial impedance model, $G$is the sensitivity (derivative) matrix, and $\Delta M$ is the model update.

## RESULT & DISCUSSION

The inversion process was performed using HRS version 11, and the resulting acoustic impedance model was systematically validated against the seismic traces. Inversion errors were quantified and iteratively minimized to achieve an optimal seismic-to-well tie (R. Simm, & Bacon, M. 2012). All workflow steps described in the subsequent section were performed within the Hampson-Russell environment.

### Horizon selection

The horizons in the X Field were interpreted inside of a chronostratigraphic framework, aligned by the regional geological history. Stratigraphic correlation suggests the main reservoir lies inside of Oligocene deposits composed of fine sandstone, calcareous shale, and mudstone. These chronostratigraphic constraints help delineate the vertical and lateral extent of the prospective reservoir units.

### Wavelet extraction

The wavelet represents the effective seismic source signature, encompassing its phase and dominant frequency content (Haris, A., Haryono, H., & Riyanto, A. 2018). Accurate wavelet estimation improves the alignment between synthetic and observed seismic data and minimizes amplitude and phase distortions that may propagate into inversion results (Sismanto, S. & Widodo, A. 2018). Studies presented in SCOG LEMIGAS highlight that deterministic wavelet extraction, based on well seismic calibration, provides more stable inputs for inversion, particularly in areas with complex geology or low-quality seismic data (Butar, M. H. P. B., Juventa, & Marlinda, L. 2023). An optimal wavelet is characterized by a zero phase signature, with symmetry and its maximum amplitude centered at time zero (HRS 2011). In the absence of check-shot data, a Ricker wavelet is typically convolved with density and sonic logs to construct a synthetic seismogram (Mavko, G., Mukerji, T., & Dvorkin, J. 2009). However, in the X Field, the availability of check shot measurements allowed for the extraction of a statistical wavelet. This wavelet was derived from the seismic volume within the 490-765 ms time window. Maintaining a symmetric wavelet is essential for ensuring proper focusing of seismic energy and achieving accurate alignment with the primary geological boundaries.

### Well to seismic tie

After statistical wavelet extraction, well tops were tied to seismic traces to achieve zero phase alignment and establish a correspondence between log markers and seismic reflections. A calibrated time–depth function was derived from check-shot data after QC of the P-wave and density logs. Previous studies have shown that consistent well ties and stable wavelet extraction can significantly improve the resolution of subsurface geological models, especially under challenging seismic conditions with limited data quality (Mavko, G., Mukerji, T., & Dvorkin, J. 2009). MAW well was

then correlated within a defined window by matching seismic and synthetic traces between the Oligocene and Eocene-3 horizons. A bulk shift, followed by stretching and squeezing, was applied to improve the match. After several trials, the MAW well achieved an R- value of approximately 63% (Fig. 1), yielding a corrected P-wave log consistent with the seismic horizons and a corresponding P- impedance transform derived using Gardner's equation.

## Crossplot analysis

The crossplot of P-impedance versus density from the MAW well shows three distinct zones, each reflecting systematic variations in elastic properties, which correlate clearly with the distribution of Gamma Ray (GR) values (Fig. 2). The first zone, located on the left side of the plot and represented by the red ellipse, is dominated by blue–cyan colors corresponding to high GR values. This pattern suggests intervals rich in shale, where fine grained minerals with higher natural radioactivity generate strong GR responses. In this zone, both P-impedance and density remain in the low to intermediate range, consistent with shale dominated lithologies that have not undergone significant compaction. The second zone, located in the central portion of the crossplot and highlighted by the blue ellipse, shows intermediate GR values, indicated by green yellow hues. This zone represents a transitional shale sand interval, where an increase in compaction and a reduction in shale content lead to progressively higher impedance and density. The mixed lithological nature of this zone reflects gradual changes in grain composition and porosity, resulting in elastic properties that bridge the contrast between shale rich sediments and cleaner siliciclastic units.

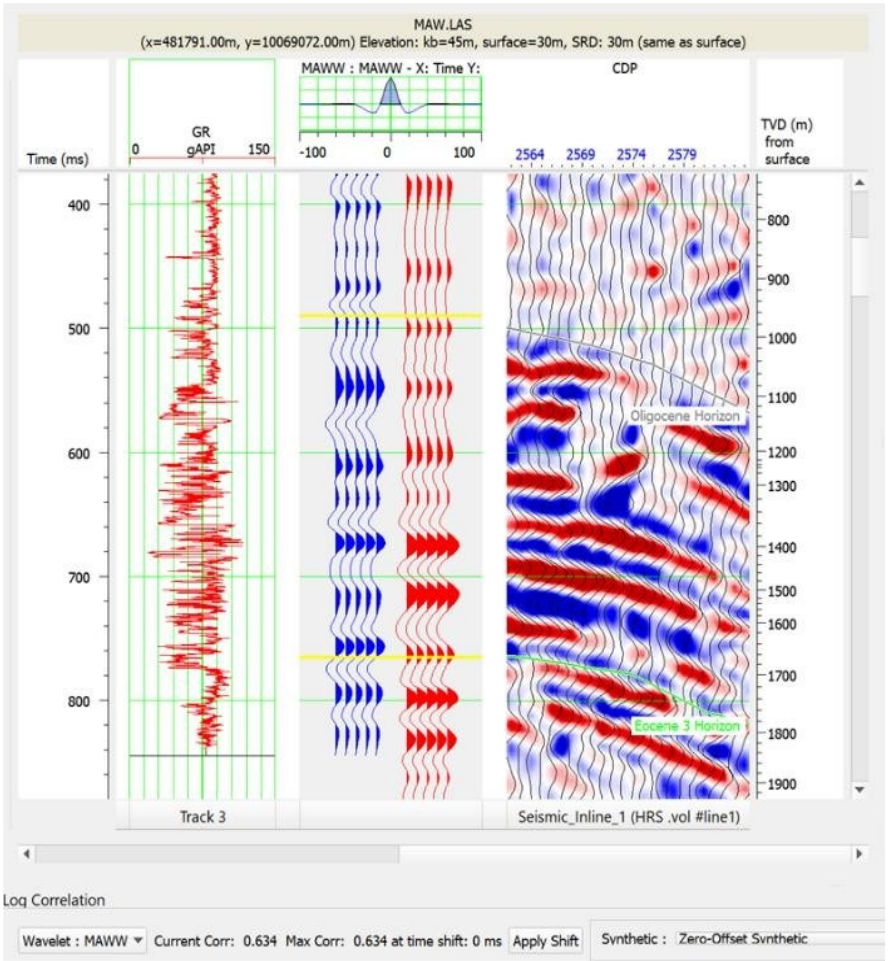


Figure 1. Snapshot of the MAW well illustrating the well– seismic tie results, with a correlation coefficient of 63.4%, reflecting a moderate level of consistency between the synthetic seismogram and the observed seismic data.

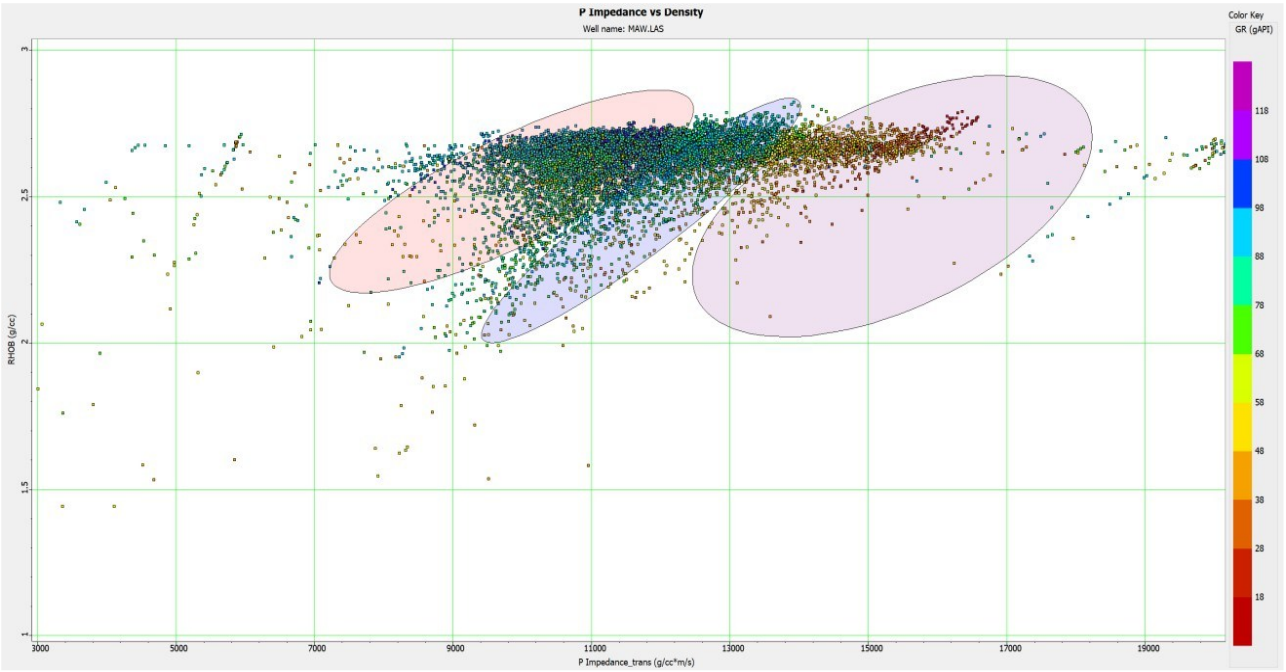


Figure 2. P-impedance versus density crossplot from the MAW well, colored by Gamma Ray values, delineating three elastic zones associated with shale-dominated, transitional, and clean sandstone lithologies. Higher Gamma Ray values cluster within the shale-dominated domain, whereas lower Gamma Ray values correspond to the cleaner sandstone interval, indicating a systematic relationship between elastic properties and lithological variation.

The third zone, located on the right side and highlighted by the green ellipse, exhibits the highest impedance and density values accompanied by red–yellow colors indicative of low GR responses. This configuration indicates the presence of clean, compacted sandstone with minimal shale content. The combination of high density and high impedance, together with low GR values, confirms a predominance of coarse grained minerals and reduced matrix effects. Collectively, the three zones demonstrate a consistent lithological trend, ranging from shale rich sediments through transitional facies to clean, compacted sandstone, providing a robust basis for elastic facies classification and for identifying reservoir quality intervals within the studied formation.

## Initial model

The P-impedance transform log is used as the primary input for constructing the initial low frequency model. This model is generated by producing a band limited impedance volume through the convolution of seismic traces with a band limited operator (R. Simm, & Bacon, M. 2012). In this study, the standard post stack acoustic impedance inversion setup was applied using a single well, which provided the density, P-wave velocity, and P-impedance logs. The modeling interval extended from 0 to 5000 ms and was constrained by the two interpreted horizons. The correspondence between the inverted and logged impedance is primarily influenced by the low frequency cut off applied to the initial model (R. Simm & Bacon, M. 2012). In HRS, a low-pass filter was used, allowing frequencies below 10 Hz to pass while attenuating those above 15 Hz (HRS 2011).

## Pre-inversion analysis

The pre-inversion model shows high quality, with a correlation value of 0.9976 between the synthetic and seismic data (Fig. 3). This result shows that the extracted wavelet accurately represents the dominant frequency and phase characteristics of the seismic signal. The low error value of 0.0693, along by the absence of systematic error patterns, further confirms that the low frequency model is stable and suitable for supporting the inversion process. The main stratigraphic horizons, including Eocene 2, Eocene 3, Oligocene, and Early Miocene, are consistent by the reflection patterns observed in the seismic data.

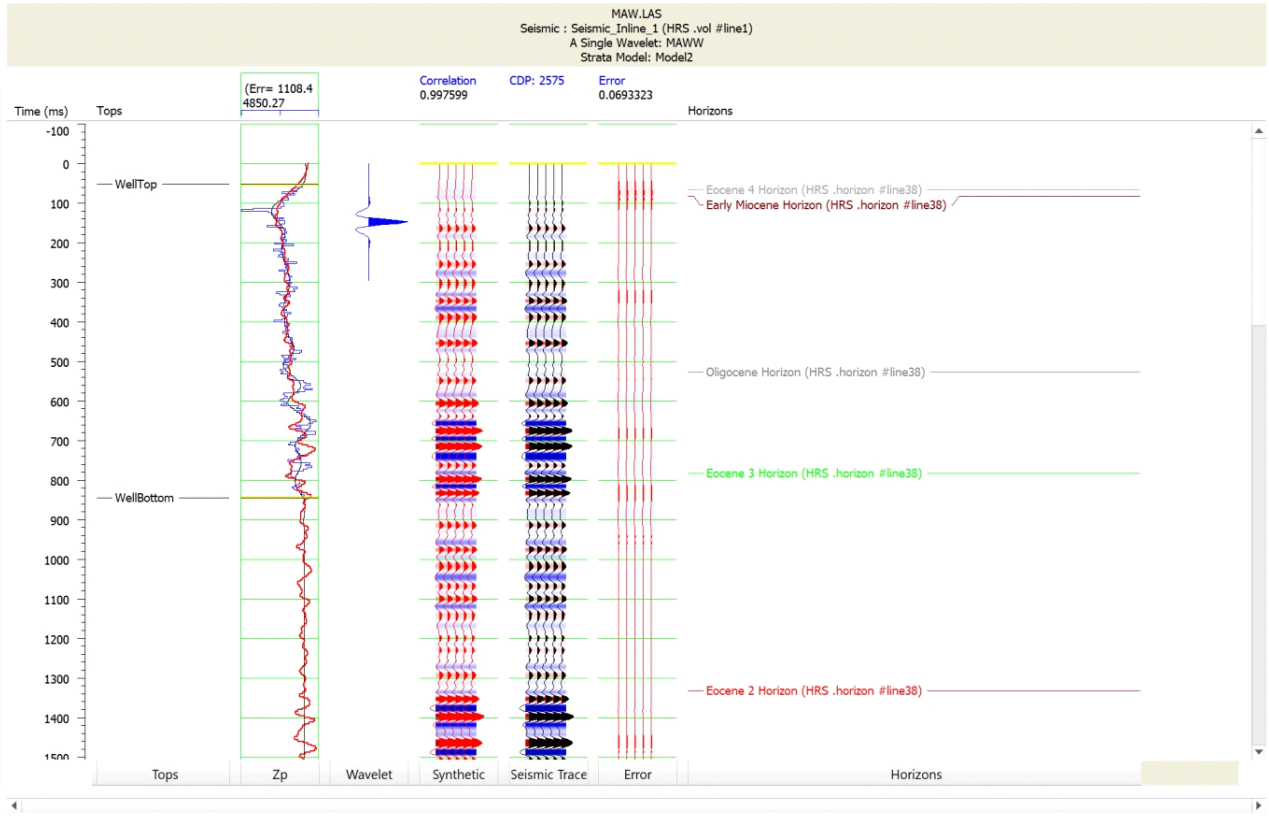


Figure 3. Pre-inversion analysis illustrating the seismic–synthetic correlation and associated error, indicating a high-quality low-frequency model and a well-defined stratigraphic framework for inversion. The strong alignment between the synthetic and seismic traces, reflected by a high correlation coefficient and low error value, confirms the reliability of the well–seismic tie and supports the use of the model for subsequent deterministic inversion.

This coherence suggests that the geological framework before inversion is well defined, providing a solid foundation for subsequent elastic modeling.

The target interval, located between the Oligocene and Eocene horizons, shows a consistent amplitude pattern and reveals a significant impedance contrast. This makes the interval an important focus for model based inversion, as it offers the potential to refine the characterization of reservoir quality and lithological variations within the zone.

### Inversion analysis

After building the initial model, an inversion analysis was performed to identify the optimal inversion parameters. The inversion was initially tested at the well location for quality control and parameter refinement K. J. Marfurt 2006, during which automatic scaling factors were generated to match the seismic amplitudes with the synthetic response.

## P impedance model based

P-impedance inversion (Fig. 4) in this study was performed on seismic inline 1, with constraints from the MAW well. The analysis focuses on the interval between the Oligocene Horizon and the Eocene 3 Horizon. This interval was chosen based on well data suggesting the presence of a reservoir zone between 490 and 765 milliseconds, making it the primary target for detailed subsurface evaluation. The model based inversion results show that the overall P-impedance (Zp) values range from 11022 to 15343 g/cc·m/s, while the target interval exhibits P-impedance values between 11500 and 15000 g/cc·m/s. Within the inversion section, the 490–765 ms interval is predominantly represented by yellow Tonal variations, which suggest the presence of moderately porous sandstone Mavko, G., Mukerji, T., & Dvorkin, J. 2009. This lithology typically shows P-impedance values around 12,000 g/cc·m/s and is often associated with depositional environments influenced by deltaic to fluvial sedimentation processes.

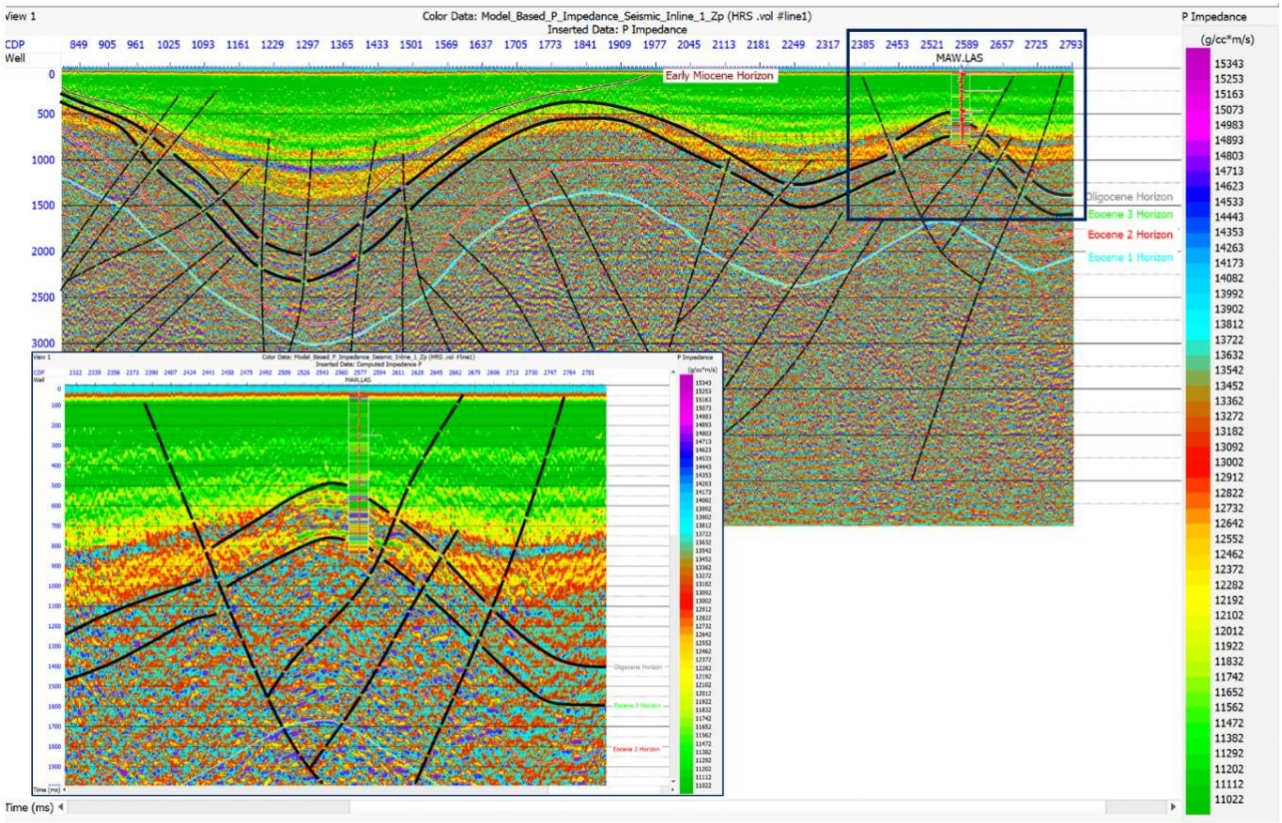


Figure 4. Model based P-impedance inversion along seismic inline 1 constrained by the MAW well, highlighting the target interval between the Oligocene and Eocene 3 horizons characterized by moderate P-impedance values indicative of porous sandstone.

Structural enhancement in the inversion section is primarily observed where impedance contrasts consistently follow and sharpen the geometry of the Interpreted seismic horizons and faults (black lines) are particularly noticeable along fold crests and flanks, where horizon continuity is improved, and at fault zones, where clearer impedance discontinuities highlight stratigraphic offsets between structural blocks. This enhancement is a result of deterministic inversion, which produces a quantitative impedance model that suppresses wavelet and tuning effects, thereby improving the definition of structural boundaries and subsurface geometry.

**Density model based**

The model based inversion results show density values ranging from 2.37 to 3.00 g/cc (Fig. 5) along the seismic line. The target interval, however, exhibits a more focused range, with values between 2.4 and 2.8 g/cc. In the 570–770 ms window, this interval is expressed predominantly by yellow to red tonal variations, which provide a visual indication of relatively compacted sandstone (Asquith, G. & Krygowski, D. 2004). These colors represent density values commonly found in sandstone that has experienced significant compaction due to burial. This process leads to moderate reductions in porosity and an overall increase in grain to grain contact.

The lithological interpretation based on density is further supported by the corresponding P-impedance values, ranging by 11,500 to 15,000 g/cc·m/s, that indicate acoustic velocities typical of consolidated clastic material. When considered together, the density and impedance patterns delineate a sandstone unit by sufficient rigidity and acoustic contrast to be distinguished by surrounding lithologies. This combination of attributes points to a laterally continuous clastic body with reservoir potential, in line with sedimentation processes that typically form sandstone rich sequences in deltaic to fluvial depositional environments.

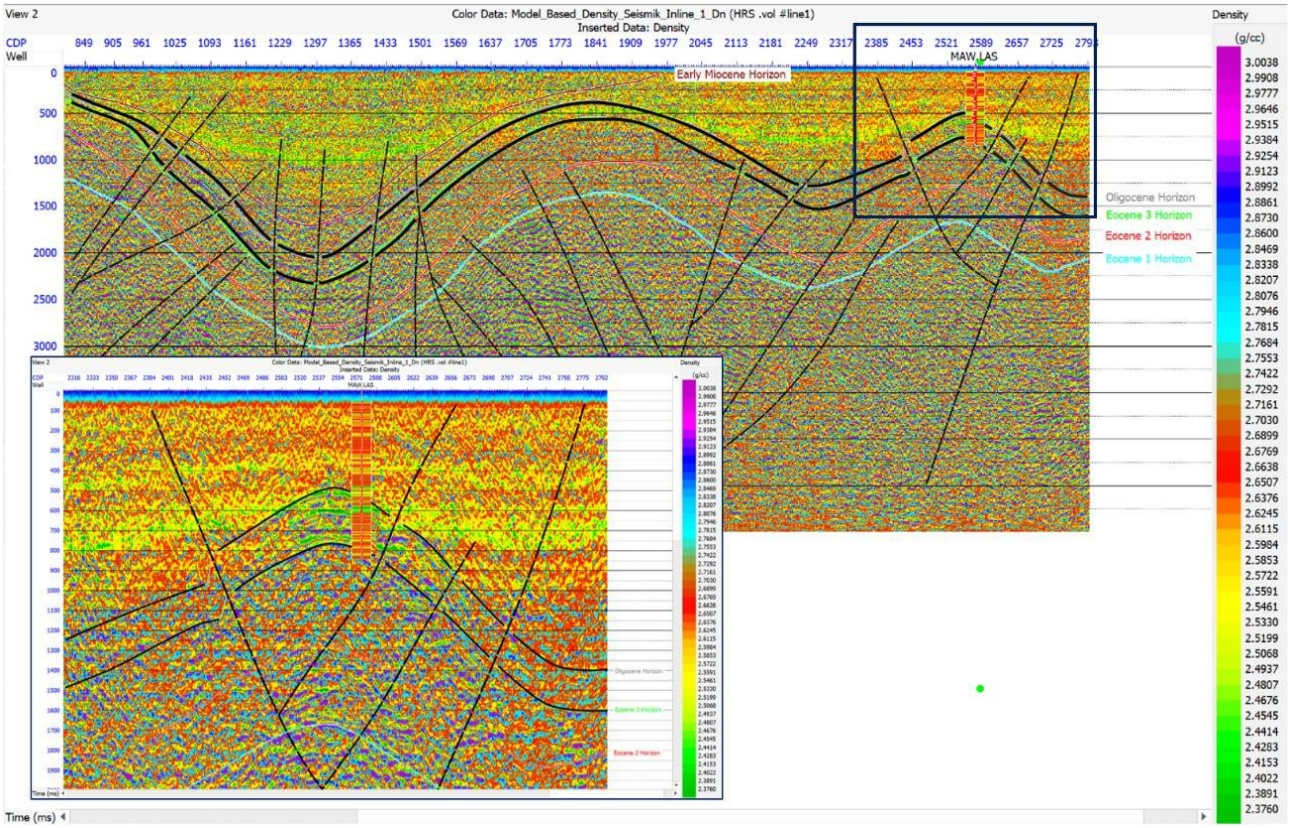


Figure 5. Model-based density inversion along seismic inline 1 constrained by the MAW well, showing elevated density values within the target interval that are characteristic of compacted sandstone and support its reservoir potential.

## Porosity model based

The porosity model based inversion results (Fig. 6) show that porosity within the analyzed interval ranges from 11% to 23%, highlighting a notable degree of petrophysical variability along the seismic section (Rose Firdiany N. S., Mohammad Syamsu R., & Edy W. 2025). Within the designated target zone, porosity values narrow to approximately 13–21%, consistent with moderately porous sandstone that retains appreciable pore space due to limited compaction. These porosity estimates are consistent with the previously derived P-impedance and density trends, where relatively lower impedance and slightly reduced density indicate a coarser grained, more porous lithology compared to the surrounding intervals (Yilmaz, Ö. 2001). However, Inside of the 490–765 ms window, porosity shows greater heterogeneity and a tendency toward reduced stability, potentially associated with facies transitions, increased clay content, or diminished seismic data quality at these times Avseth, P., Mukerji, T., & Mavko, G. 2005. As a result, the porosity estimates in this interval carry more uncertainty compared to those in the primary target zone Dubois, G. & Brossier, R. 2018.

### Apply to volume

Several parameters were assessed to evaluate the quality of the deterministic inversion, including the synthetic seismic error plot and the impedance predictions at the well. The error plot represents the difference between the input reflectivity and the synthetic section generated from the inverted impedance. Low error values indicate high inversion fidelity and the absence of undesired coherent energy.

### Quality control

Deterministic inversion often produces smoothing effects, which can bias volume estimates and obscure connectivity in thin bedded reservoirs (Sancevero, S.S., Remacre, A.Z., de Souza Portugal, R., & Mundim, E.C.

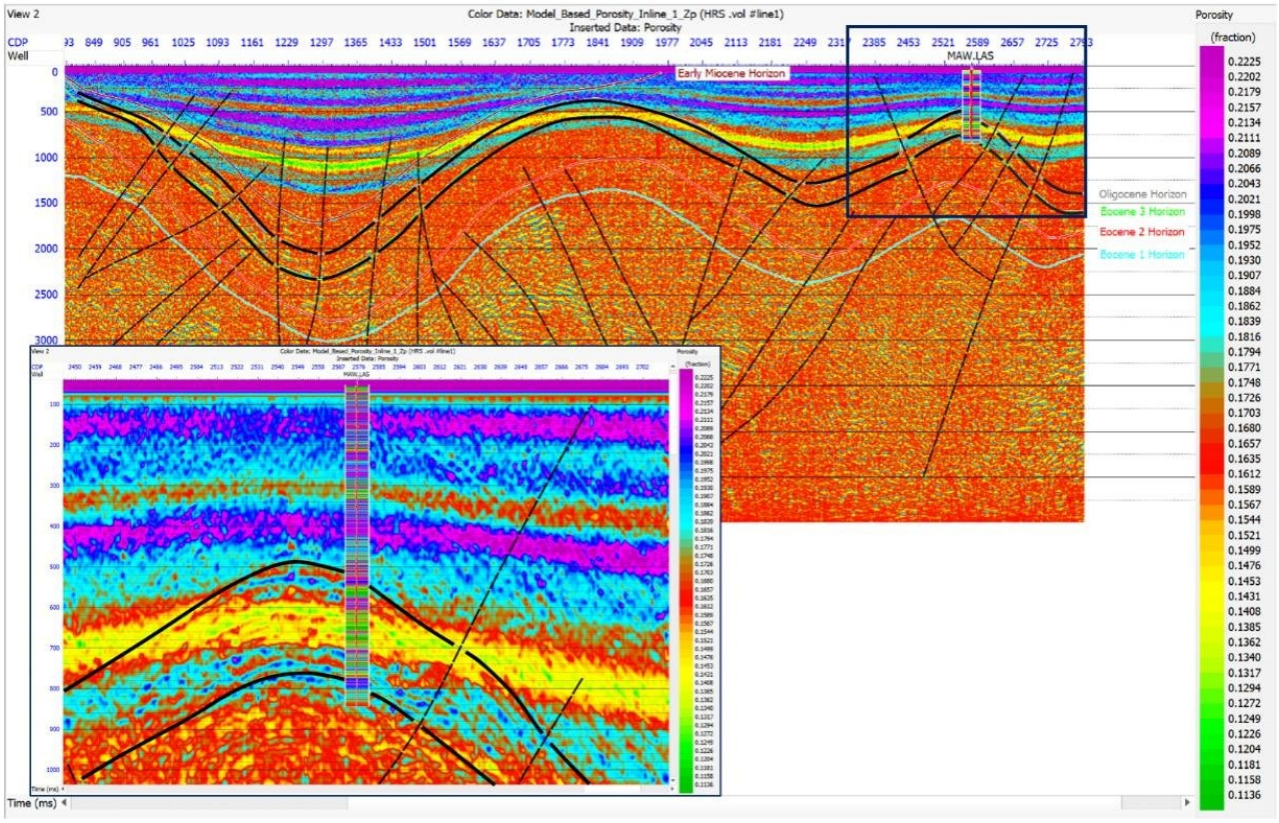


Figure 6. Model based porosity inversion along seismic inline 1 constrained by the MAW well , showing moderate porosity within the target interval that correlates with the P-impedance and density models, while exhibiting increased heterogeneity toward deeper time windows.

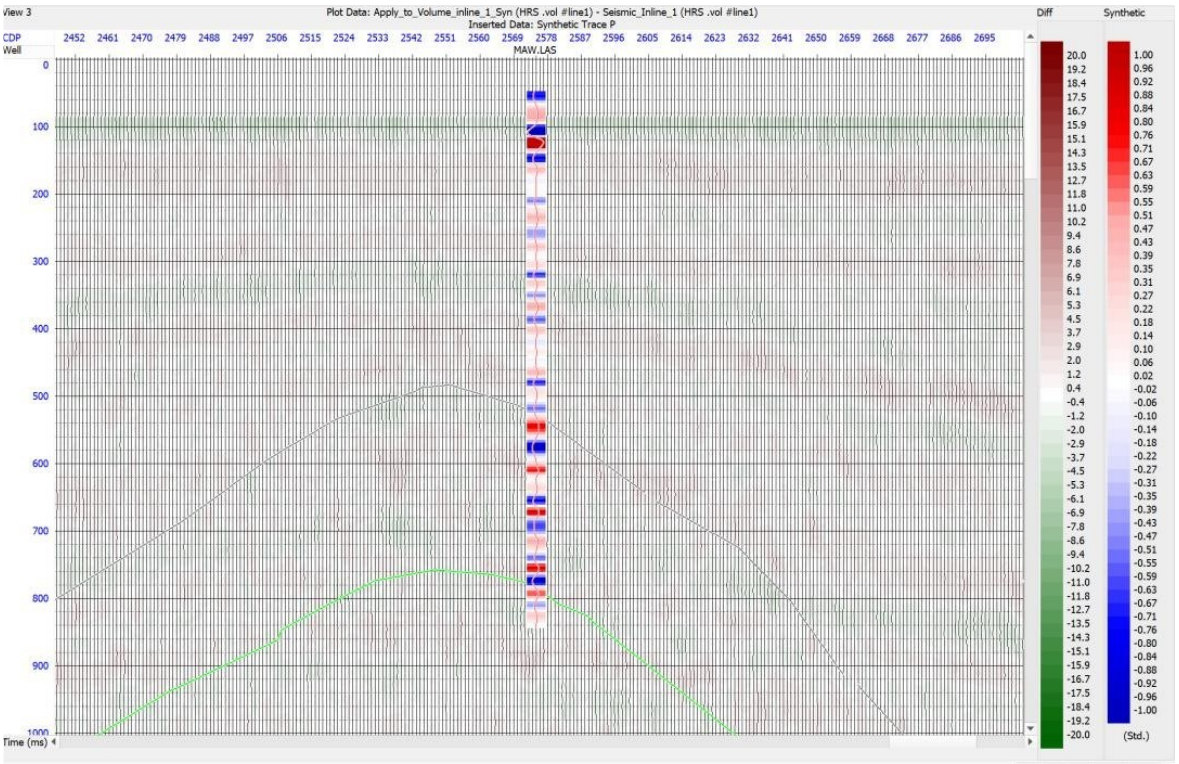


Figure 7. Comparison between synthetic and observed seismic data along seismic inline 1 constrained by the MAW well, showing a high level of agreement within the target interval, limited amplitude differences, and blind-well validation that confirms the reliability of the inversion results.

2005). To assess the reliability of the inversion results, several diagnostic parameters were analyzed, including synthetic seismic misfit and well- based impedance prediction.

An analysis of the comparison between synthetic and observed seismic data (Fig. 7) shows that the differences, represented by the Diff column, exhibit maximum deviations of ±20 units, with the majority of values within ±5, as indicated by the pink and light green colors. Within the target interval of 490–765 ms, synthetic amplitudes generally follow the trends of the observed seismic data, with only minor phase or amplitude shifts, while higher deviations occur at isolated spikes, rarely exceeding ±10. Based on visual assessment and based on standard deviation patterns, the average error between synthetic and observed data is estimated to be around 5–7%, indicating a satisfactory level of fit. Regions by deviations above ±10 appear sporadically and are mostly located outside the target zone, implying minimal impact on reservoir interpretation. Overall, the strong correlation among synthetic and observed seismic data inside of the target interval highlights the reliability of the inversion model for petrophysical analysis and reservoir characterization, although localized mismatches may occur due to seismic noise or resolution limitations. In addition, a blind-well test (MAW) was performed to assess model robustness, demonstrating consistent impedance prediction. At the well locations, the inverted impedance matches approximately 80% of the corresponding log derived impedance values, suggesting a strong correlation between the well synthetics and the seismic reflectivity within the reservoir interval.

## CONCLUSION

The outcome of this study show that model based deterministic inversion effectively improves geological resolution in areas by limited seismic data quality. The inversion generated impedance, density, and porosity models that closely match seismic observations and well log measurements, enabling reliable lithological characterization and delineation of prospective intervals. P-impedance values range by 11,022 to 15,343 g/cc·m/s, and density values range from 2.37 to 3.00 g/cc, narrowing to 11,500 to 15,000 g/cc·m/s and 2.4 to 2.8 g/cc inside of the target zone, consistent by medium to coarse grained sandstone. Porosity estimates of 13 to 21 percent indicate a moderate quality reservoir retaining adequate pore space despite compaction. Variability inside of the 570 to 770 ms interval reflects facies heterogeneity and reduced seismic resolution, leading to increased uncertainty. Nevertheless, the integrated inversion conventional seismic interpretation relies on qualitative analysis of reflection amplitudes and geometries to delineate subsurface structures. The effectiveness of conventional seismic interpretation is limited by the indirect and band limited nature of seismic responses, often leading to interpretational ambiguity in structurally complex settings. Deterministic seismic inversion provides a substantially clearer geological framework, with structural enhancement manifested in improved fault delineation, clearer structural closures, and increased continuity of reservoir- level horizons Triyoso W., Sinaga E.I., & Oktariena, M., 2004. By transforming seismic data into quantitative acoustic impedance models, this approach mitigates wavelet and tuning effects, while enhancing structural and petrophysical resolution in challenging data conditions.

## ACKNOWLEDGEMENT

The authors acknowledge the Center for Oil and Gas "LEMIGAS" for granting permission to publish the data used in this study. The authors also extend their appreciation to the Faculty of Mathematics and Natural Sciences, Universitas Indonesia (FMIPA UI) for the institutional support provided throughout the research process. Special thanks are given to Dr. Edy Wijanarko for supplying the essential dataset and for his support in facilitating the publication of this work.

## GLOSSARY OF TERMS AND SYMBOLS

| Terms & Symbols | Definition | Unit |
|---|---|---|
| Zp | P-wave impedance | g/cc*m/s |
| GR | Gamma ray | API |
| QC | Quality control | - |
| HRS | Hampson russell software | - |
| R | Coefficient of correlation | - |

## REFERENCES

Asquith, G. & Krygowski, D., (2004), Basic Well Log Analysis, American Association of Petroleum Geologists (AAPG), Tulsa.

Avseth, P., Mukerji, T., & Mavko, G., (2005), 'Quantitative Seismic Interpretation: Applying Rock Physics Tools to Reduce Interpretation Risk', Cambridge University Press, Cambridge.

Butar, M. H. P. B., Juventa, & Marlinda, L., (2023), Identifikasi prospek reservoir hidrokarbon menggunakan inversi impedansi akustik pada Blok Kampar. Lembaran Publikasi Minyak dan Gas Bumi (LPMGB), 57(1), 43–59. https:// doi.org/10.29017/LPMGB.57.1.1324.

Bosch, M., Mukerji, T., & Gonzalez, E. F., (2010), Seismic inversion for reservoir properties combining statistical rock physics and geostatistics, Geophysics, Society of Exploration Geophysicists.

Dewan, J.T., (2001), Essentials of Modern Open-Hole Log Interpretation, PennWell Publishing, Tulsa.

Dubois, G., & Brossier, R., (2018). Uncertainty quantification in seismic inversion. Geophysics, 83(4), R413–R426. https://doi.org/10.1190/geo2017-0552.1

Grana, D., (2017), 'Bayesian inversion of seismic data for reservoir characterization', Geophysics, Society of Exploration Geophysicists.

Grana, D., & Della Rossa, E., (2010), Seismic inversion using statistical rock physics models, Geophysics, Society of Exploration Geophysicists.

Haris, A., Haryono, H., & Riyanto, A., (2018). Spectral decomposition technique based on STFT and CWT for identifying the hydrocarbon reservoir. Scientific Contributions Oil and Gas (SCOG), 40(3), 125–131.https://doi.org/10.29017/ SCOG.40.3.50.

HRS, (2011), Hampson Russel Guide', pp.1–62.

H. Wu, 2015, 'Deterministic and stochastic inversion techniques used to predict porosity: A case study from F3-Block' Michigan Technological University, USA.

K. J. Marfurt, (2006), 'Robust spectral decomposition for seismic attribute analysis', Geophysics, Society of Exploration Geophysicists.

Mavko, G., Mukerji, T., & Dvorkin, J., (2009), The Rock Physics Handbook: Tools for Seismic Analysis of Porous Media, Cambridge University Press, Cambridge.

R. Simm, & Bacon, M, 2012, Seismic amplitude: An interpreter's handbook, Cambridge University Press, New York

Robinson, E. A., & Treitel, S., 2000. Geophysical Signal Analysis, Society of Exploration Geophysicists.

Russell, B. H. 1988. Introduction to Seismic Inversion Methods. Society of Exploration Geophysicists (SEG), Tulsa.

Sancevero, S.S., Remacre, A.Z., de Souza Portugal, R., & Mundim, E.C., 2005, 'Comparing deterministic and stochastic seismic inversion for thin-bed reservoir characterization in a turbidite synthetic reference model of Campos Basin, Brazil', The Leading Edge, 24, 1168–1172.

Sheriff, R. E., & Geldart, L. P. 1995.

Exploration seismology (2nd ed.). Cambridge University Press.

Rose Firdiany Nur Sukma, Mohammad Syamsu Rosid, & Edy Wijanarko, (2025), Telisa Formation Characterization Using Seismic Acoustic Impedance Inversion in the Akasia Area of the Central Sumatra Basin. Scientific Contributions Oil and Gas (SCOG), 48(2), 29–40. https://doi.org/10.29017/scog.v48i2.1774.

Triyoso, W., Sinaga, E. I., & Oktariena, M., (2024), Seismic data processing and seismic inversion in the ray parameter domain: Common reflection point (CRP) stack and ray impedance. Scientific Contributions Oil and Gas, 47(2), 129–139. https://doi.org/10.29017/SCOG.47.2.1621

Yilmaz, Ö., (2001), Seismic Data Analysis: Processing, Inversion, and Interpretation of Seismic Data, Society of Exploration Geophysicists (SEG)', Tulsa.